

Whole Blood Pumping With a Microthrottle Pump

M. J. Davies,^{a)} I. D. Johnston, C. K. L. Tan, and M. C. Tracey

School of Engineering and Technology, University of Hertfordshire, College Lane, Hatfield, Hertfordshire, AL10 9AB, UK.

^{a)} Author to whom correspondence should be addressed. E-mail: m.davies@herts.ac.uk

We have previously reported that Microthrottle Pumps (MTPs) display the capacity to pump solid phase suspensions such as polystyrene beads which prove challenging to most microfluidic pumps. In this paper we report employing a Linear Microthrottle Pump (LMTP) to pump whole, undiluted, anticoagulated, human venous blood at $200 \mu\text{l}\cdot\text{min}^{-1}$ with minimal erythrocyte lysis and no observed pump blockage. LMTPs are particularly well suited to particle suspension transport by virtue of their relatively unimpeded internal flow-path. Micropumping of whole blood represents a rigorous real-world test of cell suspension transport given blood's high cell content by volume and erythrocytes' relative fragility. A modification of the standard Drabkin's method and its validation to spectrophotometrically quantify low levels of erythrocyte lysis by haemoglobin release is also reported. Erythrocyte lysis rates resulting from transport via LMTP are determined to be below one cell in five hundred at a pumping rate of $102 \mu\text{l}\cdot\text{min}^{-1}$.

Introduction

Blood Transport in Microfluidics

Interest in blood cell transport and analysis in microfluidic devices extends back to the early 1990s and involved the development of precision cell-mechanical characterisation systems for biomechanical studies. The earliest application is by Kikuchi et al¹ who reported a simple silicon micromachined flow cell used in the manner of a microfilter. We subsequently reported the use of a silicon-glass flow cell in conjunction with real-time image processing to yield cell-by-cell cytomachanical indices for erythrocytes². This research continued with the development of a complete instrument³ that was eventually employed to analyse limited clinical samples for medical conditions including Thalassaemia⁴. The authors' past experience in developing this relatively automated analysis system underlined the need for the careful handling of blood in order to avoid erythrocyte lysis within the microfluidics. Other related micromachined flow cells for cytomachanical studies, albeit without such extensive supporting instrumentation, were developed⁵. Papers have continued to appear in this area in more recent years⁶⁻⁹.

The first report of blood transport by micropumping techniques was by Furdui et al¹⁰ who adapted an electrolysis driven micropump¹¹ resulting in a single delivery, 'one-shot', blood micropump employing gas bubble generation to displace a $7\mu\text{l}$ volume of blood into an analysis area. Recently, a triple actuator, silicon-glass, peristaltic pump for transport of blood samples has been reported¹². The authors described the use of a self assembled monolayer to inhibit the binding of platelets to the silicon surface which might otherwise cause leucocyte activation. The authors proceed to report maximum blood pumping rates of $50 \mu\text{l}\cdot\text{min}^{-1}$ and back pressures of 1.8 kPa which were significantly lower than the corresponding values obtained with water due to the increased viscosity of the analyte.

The use of elastomeric microfluidic devices for other areas of blood cell handling^{8,13,14} is becoming more common due to lower fabrication costs, ease of manufacture and biocompatibility¹⁵. As a result of these developments several composite micropumps, developed to be able to pump blood, have been reported incorporating elastomer as a fluid contact material^{16,17}. The elastomer/glass composite micropump reported here, while not initially designed for biomedical purposes, utilises all of these features.

Microthrottle and MTP Operating Principles

As previously reported¹⁸, Microthrottle Pumps (MTPs) were developed to utilise ‘throttling’: the use of variable cross-section flow-constrictions (microthrottles) to control fluid flow¹⁹. A detailed discussion of microthrottles, their application in microthrottle pumps and the operating principles of microthrottle pumps, has been made previously²⁰, therefore only a brief summary is provided here. Microthrottles necessitate the use of an elastomeric material to enable the formation of a variable cross-section microchannel segment. Previous observations have confirmed, in agreement with Finite Element Modelling (FEM), that the microthrottle surfaces do not contact²¹ and, as intended, exhibit quite modest closed to open flow resistance ratios (8:1 in the latest throttle designs²¹). However, despite their modest ratios, relative to conventional, fully closing valves, pumps incorporating a pair of such throttles demonstrate pumping efficiencies close to those of micropumps incorporating conventional, fully-closing valves²⁰. In addition, as a result of the lack of full throttle closure, pumps utilising microthrottles have been demonstrated to be tolerant of high particle concentrations²² and are not affected by interfacial stiction, which is commonly exhibited if PDMS contacts another surface²³, and are therefore capable of operating at high actuator frequencies (circa 1800 Hz), in the context of PDMS devices.

Microthrottle Pumps (MTPs)

Microthrottle Pumps utilise two microthrottles placed at the nodal (central) and anti-nodal (peripheral) points of a single piezoelectric bimorph-disc driven actuation layer (Figure 1). Each pumping cycle occurs as a result of the constriction of the peripheral microthrottle with simultaneous expansion of the pump chamber (suction stroke). This is followed by constriction of the central microthrottle and compression of the pump chamber, with simultaneous opening of the peripheral microthrottle creating a low fluid resistance output path (pump stroke).

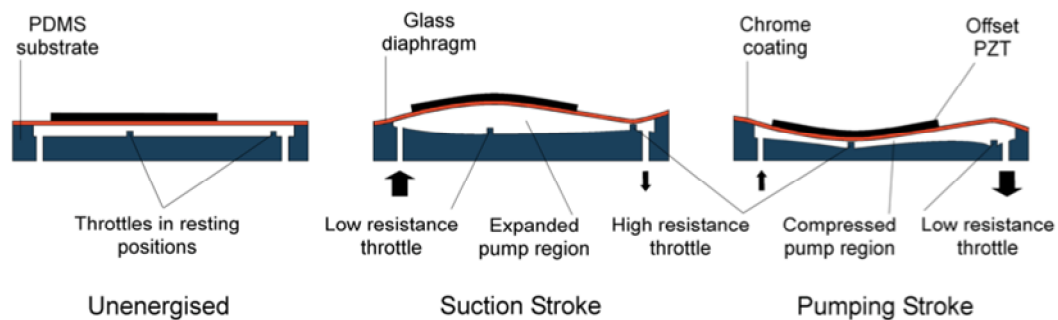


Figure 1. Schematic of a single piezoelectrically actuated, double depth MTP operating cycle. The direction of pumping through the device is left to right.

Significant development of MTPs has occurred to enhance their operation. This evolution of MTPs has been presented previously²⁴, and hence is only summarised here. Initial variants of the microthrottle pumps incorporated a defined pump chamber with throttles constricting normal to the axis of compression²². Subsequent developments included the use of throttles constricting parallel to the axis of compression implemented within double-depth structure²², providing enhanced throttling ratios via displacement

amplification²⁰, and the utilisation of the inter-throttle region of the pump channel as the pump chamber²¹, thereby reducing undesirable recirculatory effects within pump chambers as reported by Andersson et al²⁵. The resulting Linear Microthrottle Pumps (LMTP) demonstrated pumping rates up to 1.4 ml.min⁻¹ and the ability to pump against a back pressure of 35 kPa of water²¹.

Fabrication and Assembly

The LMTP employed here has an optimised 1 mm wide, 100 µm deep channel with 20 µm deep throttles, that is thus slightly different to those we have characterised and reported previously²⁴. The refinement in this variant primarily involves a slightly increased throttle gap in order to ensure that erythrocyte's are not 'pinched' in the compression stroke and thus potentially lysed. The overall device is of identical dimensions and employs an identical PZT (see definition below) bimorph actuator to previous MTPs.

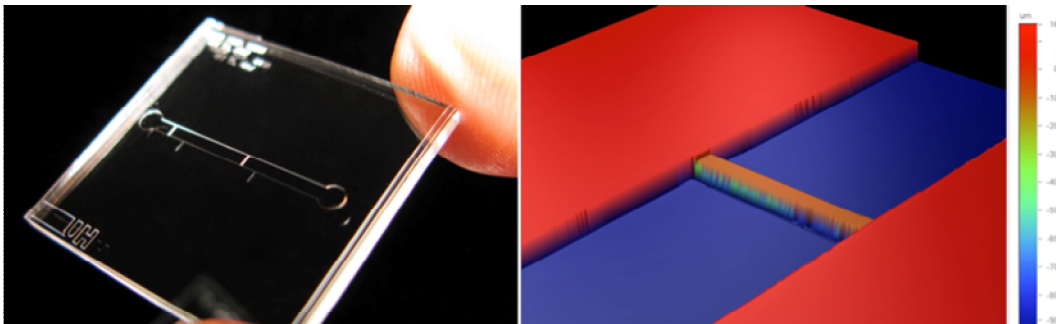


Figure 2. PDMS LMTP substrate. Left is a photograph of the LMTP casting focusing on the structure while the right hand image shows a surface profile of one of the double depth throttles employed in the design. Also included in the surface profile image is the depth information provided by the surface profiler.

The LMTPs were fabricated and assembled in the manner we have previously described in detail²⁰, which is briefly summarised here. Molds were microfabricated from SU8 (Microchem Corp.) structural photoresist on silicon wafers. The PDMS microstructures were then cast in Dow Corning Sylgard[®] 184 PDMS processed in the, previously reported¹⁸, standard way (Figure 2). The LMTP was then assembled. Firstly a glass microscope slide was cut to size to form a back-plate and diamond drilled to provide fluid vias. A cover slip was then coated with chromium, by evaporation, to facilitate electrical connection to the piezoelectric actuator. The PDMS, cover slip and back-plate were then UV-Ozone treated, bonded, assembled and then baked at 90°C for 2 hours. The PZT (lead zirconate titanate) piezoelectric bimorph disc (Piezo Systems, T216-A4NO-273X) was then bonded to the cover slip with conductive epoxy adhesive and fine connecting wires were attached. An assembled LMTP is shown in Figure 3.

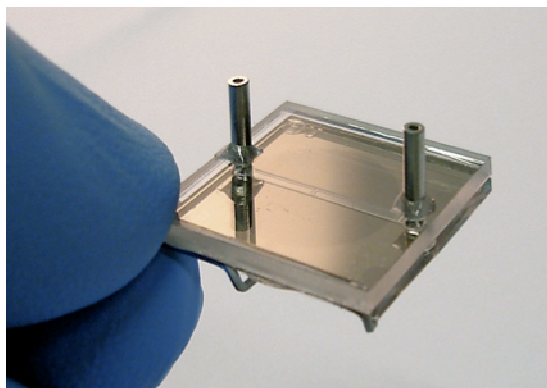


Figure 3. An assembled LMTP.

Blood Pumping Evaluation

Blood Preparation

Venous blood, taken from a single donor, was drawn into two 9 ml EDTA vacutainers (Griener Bio-one, Austria). Care was taken to immediately agitate the sample in order to thoroughly disperse the precoated EDTA anticoagulant. The contents of the vacutainers were combined, to ensure that inter-sample differences were eliminated, and kept at room temperature.

The whole blood was then separated into two aliquots. One aliquot for evaluation of the flow rate vs frequency performance of the LMTP and one aliquot for further division as required to provide samples for determination of the percentage erythrocyte lysis of the LMTP at selected actuator frequencies and voltages. Prior to all measurements the blood to be pumped was agitated gently to ensure an even suspension of all cellular material. Greater volumes of blood were contained within the fluid input reservoir than were required for each experiment. This, combined with the diameter of the tubes used, the position of the input tube and the calculated maximum erythrocyte sedimentation rate of 15 mm/hr for the donor²⁶ indicated that cell sedimentation was insignificant over the experimental time period. Therefore no agitation was required during individual experiments. Following measurement of the flow rate / actuator frequency relationship, three samples were taken from the second aliquot of whole blood, with each being taken immediately prior to pumping, for measurement of percentage erythrocyte lysis. As each sample was removed from the second aliquot for pumping, a second, identically sized, sample was removed and placed into a microcentrifuge tube to act as a reference sample for subsequent differential spectrophotometric comparison with the pumped sample to determine pump-induced lysis.

Experimental System

All characterisations of pump performance were performed by mass transfer of either filtered DI water or freshly drawn, anticoagulated, whole blood from a reservoir placed on a precision microbalance (Sartorius 210s, Sartorius AG) with data processed in real time by software written in LabVIEW® (National Instruments) to obtain mass flow rate values. The volumetric flow rate was then calculated from the measured mass flow rate using a blood density of 1.05 g/ml at a room temperature of 22°C²⁷. Fluid system preparation was as previously described²², however priming was performed with filtered, degassed phosphate buffered saline (PBS) rather than deionised water to avoid cell lysis at the interface between incoming blood and the priming solution. The initial flow of blood through the fluid system was continued for 30 s, prior to any measurements, to ensure the complete removal of PBS. All measurements of flow rate were conducted as previously described²² using bespoke drive electronics²¹ programmed to increase the drive frequency in increments of 100 Hz with a 30 s actuation period for each frequency. A 10 s pause between each incremental increase in frequency was included to enable confirmation that the flow rate reduced to zero following each measurement. That is, that any slight change in relative fluid reservoir and waste height did not affect the initial set starting flow condition and that the LMTP exhibited no hysteresis. Back pressure measurements were performed by measuring the rate of mass transfer from the fluid input bottle as a back pressure was applied to the fluid waste bottle following zeroing of the flow from the fluid input to fluid waste. The back pressure was finely controlled and increased incrementally via a precision needle valve (Type 91, Marsh Bellofram Corp, WV, USA) while the applied pressure was measured using a digital pressure meter (DPI 705, Druck, USA). The flow resistance of all input and output tubing was measured to enable accurate calculation of pump performance. The height change of fluid levels were calculated to have an insignificant effect on either the flow rate or back pressure measurements over the period of time that each experiment was conducted.

Supernatant Haemoglobin Measurement

The hemoglobin detection limit of the recommended International Council for Standardisation in Haematology (ICSH) standard method (1995)²⁸ (ICSH-sm95) and the World Health Organisation²⁹ was calculated to be too high for the accurate determination of haemoglobin released from lysed erythrocytes during the pumping of whole blood. Accordingly, a modified version of the ICSH-sm95 (described subsequently) was employed to determine the haemoglobin present in the whole blood sample.

Sample pre-treatment and haemoglobin analysis methodology are briefly detailed below.

Erythrocyte lysis is conveniently evidenced by the release of the erythrocytes' haemoglobin-rich stroma into the suspending (supernatant) phase. Accordingly, subsequent to pumping, the cells in both the pumped blood samples and the reference samples were spun-down in the same centrifuge operation at 2000 rpm for 2 minutes in order to rapidly sediment the cells and allow us to remove cell-free samples of supernatant.

Once the supernatant was removed from the centrifuged samples, Drabkin's reagent (Sigma-Aldrich) was added in the ratio 25.1 parts to 1 part supernatant to convert all haemoglobin to its stable cyanohaemoglobin form³⁰. After leaving to react for 5 minutes, the solution was then centrifuged for 15 minutes at 2000 rpm to sediment the majority of the cellular debris. 0.22 μm pore size, low protein interaction filters (Millex, PVDF Membrane, Millipore) were then used to remove any remaining particulate matter and cell debris. Measurements of the absorbance were then made at 540 nm using a Jenway 6300, UV/Visible spectrophotometer (Jenway, Dunmow, UK) with cuvettes having a path length of 10 mm.

All pumped and reference whole blood samples were prepared, using the methodology described above, prior to any absorbance measurements being made. This reduced the likelihood of any variation in the absorbance measurements resulting from external conditions. Following the measurement of all sample absorbances, the equation provided by Zwart et al (1996)²⁸, adjusted to account for the difference in the dilution factor resulting from modifying the ICSH-sm95, was used to calculate the concentration of haemoglobin in both the reference and the pumped whole blood samples. The difference in the calculated haemoglobin concentration between the pumped whole blood sample and the associated reference sample was then used to determine the percentage erythrocyte lysis.

Results

Blood Pumping

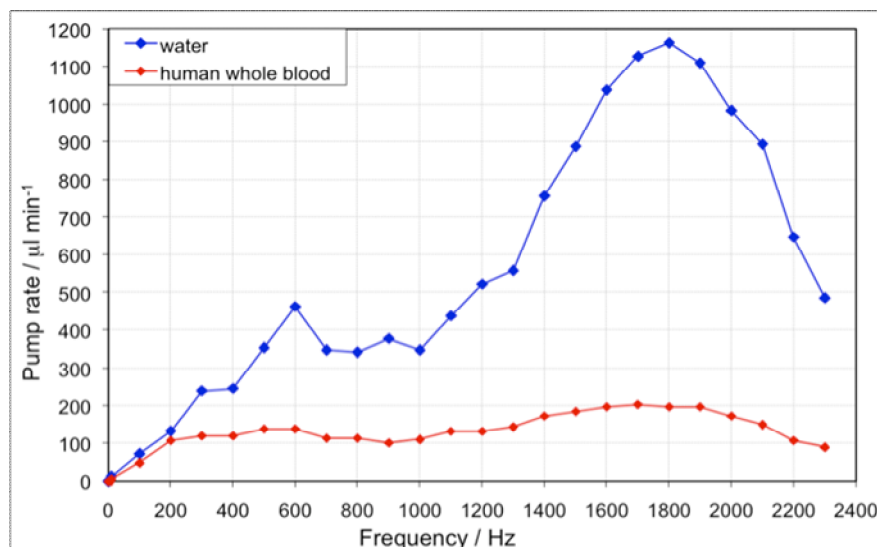


Figure 4. LMTP water and blood pumping rates as a function of drive frequency.

Figure 4 displays pumping rate as a function of driving frequency for both water and whole blood. It can be seen that the pumping rate characteristics with water are similar to those previously reported^{21,24}, with pumping rate reducing at approximately 700 Hz due to structural resonances in the LMTP device. However the pump rates achieved with whole blood display a much ‘flatter’ pump rate / frequency relationship. Maximum pumping rates of 1150 $\mu\text{l}\cdot\text{min}^{-1}$ (at 1800 Hz) for water and 204 $\mu\text{l}\cdot\text{min}^{-1}$ (at 1700 Hz) for whole blood were achieved. The ability of the LMTP to pump against a back pressure is shown in Figure 5. Although there is a considerable difference between the maximum back-pressures for water (40 kPa) and whole blood (25 kPa) the peak back-pressures, with blood, represent a considerable improvement over previously reported micropumps^{10,12}.

Blocking or gradual reduction in efficacy of the majority of micropumps and microvalves is a significant problem when the solution being pumped contains suspended phase particles^{19,31}. Micropumps, that are particle tolerant, tend not to feature completely closing microvalves as integral components due to particles preventing full closure of the valve¹⁹, thereby reducing the micropump’s efficiency. Peristaltic and non-mechanical micropumps have been developed that are capable of pumping particle laden solutions. However the reported back pressures and flow rates tend to be significantly lower than the LMTP reported here^{12,16,32,33}. As previously stated, the LMTP has been demonstrated to be able to pump a solution containing a high concentration of suspended particles²².

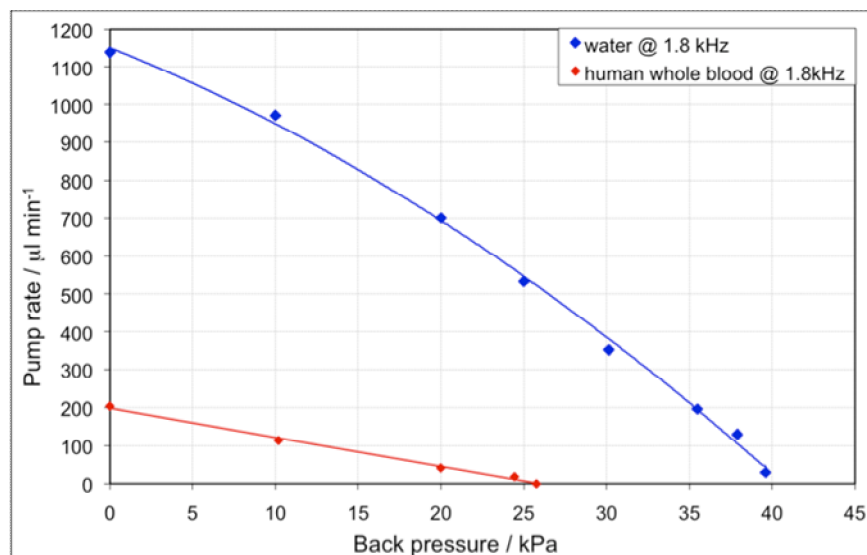


Figure 5. LMTP water and blood back-pressure as a function of drive frequency.

However, further consideration also indicates that particle tolerance does not necessarily correlate with, although it is required for, cell tolerance³³. Therefore specific attention was paid to any potential sign of blocking. During a total blood pumping time in excess of one hour no visible sign of blockage or cell adhesion was observed. That time represented all blood pumping required for the measurement of the flow rate / actuator frequency relationship and yielding samples for the percentage erythrocyte lysis calculations.

Cell Lysis

The ICSH recommends the use of Drabkin’s Reagent for analysis of free haemoglobin and almost all derivatives²⁹. A mixture of potassium cyanide, potassium ferricyanide and a non-ionic detergent, Drabkin’s reagent reacts with all haemoglobin, excepting sulphaemoglobin, to convert it to cyanohaemoglobin. Cyanohaemoglobin being more stable than haemoglobin and possessing only one spectral absorbance peak, in contrast to

the multiple peaks produced by the derivatives of haemoglobin molecules found in blood, is a more straightforward spectrophotometric analyte than native haemoglobin.

The detection limit of the ICSH-sm95 was calculated to be 1.10 g/l of cyanohaemoglobin for the spectrophotometer used: a value that was anticipated to be too high. Accordingly we modified the ICSH-sm95 by increasing the sample volume of Drabkin's reagent added to the sample, thereby reducing the dilution factor from approximately 4×10^{-3} to approximately 4×10^{-2} , resulting in a factor of 10 increase in the cyanohaemoglobin concentration and therefore absorbance, relative to the background absorbance. The modified ICSH-sm95 was validated by comparing the cyanohaemoglobin concentrations of serum samples, obtained by centrifuging and filtering whole blood, and serially diluted whole blood with those obtained using the ICSH-sm95, as shown in Figure 6. The serum samples provided representative blanks. Absorbance was observed to increase linearly with concentration for the modified ICSH-sm95 and a detection limit of 0.11 g/l was calculated for cyanohaemoglobin. This is equivalent to approximately 0.1% of the whole blood haemoglobin concentration. Results obtained by comparing the modified ICSH-sm95 and standard ICSH-sm95 differed by less than the experimental error of the ICSH-sm95 within the concentration range over which both analyses were valid.

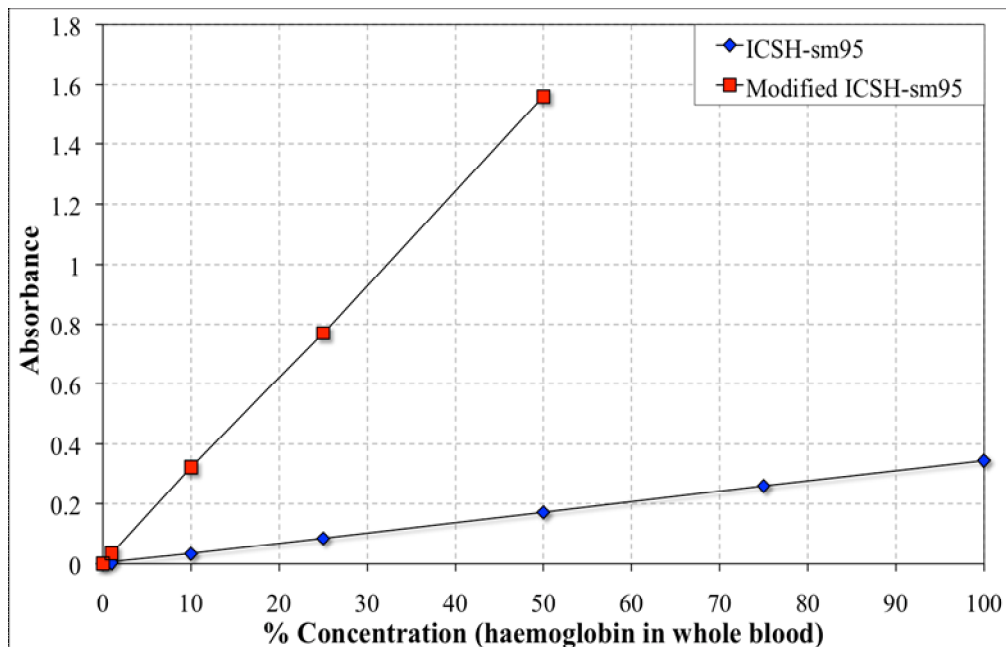


Figure 6. Calibration plots demonstrating the linear response of the absorbance, resulting from the ICSH-sm95 and the modified ICSH-sm95, to diluted whole blood. The slopes of the modified and standard methods are 0.03 and 0.003 respectively with an r^2 of 0.9999 for both. Cuvette path length was 10 mm.

Greater volumes of whole blood were required to be pumped for measurements of percentage lysis than for measurements of flow rate at each frequency. All measurements of percentage lysis demanded a minimum volume of 3 ml. Preliminary measurements were attempted using commercially available sheep blood. However erythrocyte lysis in transit was such that any lysis occurring as a result of the LMTP operation was masked. Therefore the decision was made to use human blood from a local, healthy donor. To prevent agglutination human blood obtained from a single donor within the hour prior to the measurements was used. Even at peak flow rate, pumping sufficient blood to measure percentage lysis required 15 minutes. Significant effort was made to ensure measurements were made as rapidly as possible following blood being drawn. Therefore, in order to prevent artifacts being introduced in the percentage lysis measurements, as a result of significant variation in time ex-vivo, and considering that flow rate

measurements were required to be taken prior to analysis of erythrocyte lysis, the number of measurements of percentage lysis were necessarily limited. Accordingly measurements of the proportion of erythrocytes lysed during the pumping of whole blood were made at selected drive frequencies and voltages based on previous MTP experience. Peak flow rate was observed at a drive frequency of approximately 1800 Hz and voltage of 180 V. Measurements of percentage lysis were made at the peak flow rate conditions and at half the peak drive frequency and roughly half the drive voltage to independently determine the proportional effect on erythrocyte lysis of these changes. The results obtained are presented in Table 1 below.

Drive Frequency (Hz)	Voltage (V_{pk-pk})	Percentage erythrocytes lysed	Pump Rate ($\mu\text{l}\cdot\text{min}^{-1}$)
1800	180	0.7	198
1800	100	0.2	56
900	180	0.2	102

Table 1.: Results of measurements of erythrocyte lysis following pumping at selected PZT drive frequencies and voltages.

Reducing the drive frequency from 1800 Hz to 900 Hz reduces the pumping rate by 50%, but as shown in Table 1 the proportion of lysed cells is reduced by about 70%. In comparison, a drive voltage of 100 V decreases both the pump rate and the erythrocyte lysis proportionately by about 70%.

Discussion

As Figure 4 illustrates, between pumping frequencies of (200 – 1800) Hz, a ratio of 1:9, the pumping rate of blood approximately doubles. However, water increases by approximately ten times over the same frequency range. This indicates that, when pumping rheologically Newtonian water, each pump stroke displaces a broadly constant, pump-frequency independent, volume of water. However when pumping non-Newtonian blood the displaced volume per pump stroke declines with pumping frequency (nonetheless, increasing pumping frequency slightly offsets this to result in a small net increase in pumping rate with pumping frequency).

It follows from the preceding argument that the energy invested into the pumped fluid, per volume of liquid pumped with each pump stroke, is effectively pump-rate independent in the case of water, but is strongly pump-rate dependent in the case of blood. We would expect that cell lysis is proportional to the energy invested per unit pumped volume and would be spatially concentrated in the maximum energy density liquid regions of high, time dependent, shear associated with the microthrottles. Accordingly, given the higher energy invested per unit volume of pumped blood at higher pumping frequencies, we would anticipate increased erythrocyte lysis at such frequencies. Examining erythrocyte lysis data in Table 1. we find that, for the same drive voltage, and hence energy invested per pump stroke, erythrocyte lysis more than triples with a doubling in frequency from 900 Hz to 1800 Hz. Likewise for iso-frequency conditions with increased drive voltage, and hence energy per pump stroke, erythrocyte lysis again more than triples as voltage is increased from 100 V to 180 V.

Further formal development of LMTP blood pumping would benefit from a deeper theoretical understanding of blood flow behaviour within the LMTP throttle area. This may allow an explanation of blood's pumping rate / frequency function. However, it is anticipated that this would be quite challenging in view of the microthrottle gap being comparable to a few erythrocyte diameters³², indicating that assuming bulk rheological properties for blood in the high shear region would be questionable: the dimensions, and hence anticipated micro-rheology, are comparable to the physiological microvasculature.

Formal analysis of such dynamic micro-rheological behaviour would prove challenging due to erythrocytes having a non-trivial, bi-concave, discoidal morphology³⁵ and furthermore their functionally deforming under the influence of fluid shear³⁶, thus modifying their contributions to local micro-rheology in the vicinity of the microthrottles.

Conclusions

We have demonstrated continuous pumping of whole, undiluted, anti-coagulated, venous blood in an LMTP micropump (Figure 7, enhanced). The LMTP's operation has been confirmed to be blood-compatible, in the context of cell lysis, by assessing percentage erythrocyte lysis by means of haemoglobin release into the supernatant. Analysis-limited lysis levels of less than one erythrocyte in five hundred were recorded at a pump rate of 102 $\mu\text{l}\cdot\text{min}^{-1}$. Apart from indicating low levels of cell mechanical stress as a property of this type of micropump, such low levels of lysis may be beneficial to downstream on-chip cell processing functions such as PCR: a process that is compromised by haemoglobin contamination³⁴.

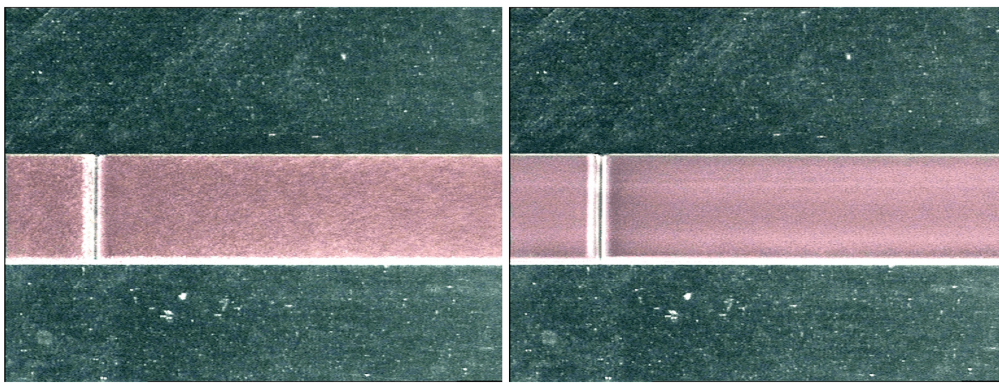


Figure 7. Still images taken from video of the LMTP prior to and during actuation. Whole blood in a 1 mm wide LMPT. Left is under static (no flow) conditions and right is flow generated by pumping at 1600 Hz. Individual cells are not visible (a result of the high cell concentration and channel dimensions) in the left hand image. However the stippled appearance of the left hand image, particularly over the microthrottle, compared to the streamlined right hand image is indicative that the blood is sufficiently static for little to no smearing to appear. The right hand image in contrast exhibits the streamline effect present in high particle concentration solutions at high flow rates. The throttle shown is the input to the chamber, i.e. the flow direction is left to right.

Acknowledgements

We would like to thank our former, now retired, colleague, John Davis, for his valuable contribution to the design and modelling of previous generations of MTPs without which this work would not have been possible. We also wish to acknowledge our colleagues, nurse Sybil Pearson, for her kind assistance in taking blood samples and Dr Dan McCluskey for his advice and proofreading of the manuscript.

References

- ¹ Y. Kikuchi, K. Sato, H. Ohki and T. Kaneko, *Microvas. Res.*, **44**, 226-240 (1992).
- ² M. C. Tracey, R. C. Greenaway, A. Das, P.H. Kaye and A. J. Barnes, *IEEE Trans. on Biomed. Eng.*, **42**, 751-761 (1995).
- ³ N. Sutton, M. C. Tracey, I. D. Johnston, R. C. Greenaway and M. W. Rampling, *Microvas. Res.*, **53**, 272-281 (1997).
- ⁴ M. C. Tracey, N. Sutton, I. D. Johnston and W. Doetzel, *1st Ann. IEEE-EMBS Special Topic Conf. on Microtech. in Med. and Biol.*, Lyon, 2000.
- ⁵ J. P. Brody, Y. Han, R. H. Austin and M. Bitensky, *Biophysic. J.*, **68**, 2224-2232 (1995).
- ⁶ W. G. Lee, H. Bang, H. Yun, J. Lee, J. Park, J. K. Kim, S. Chung, K. Cho, C. Chung, D-C. Han and J. K. Chang, *Lab Chip*, **7**, 516-519 (2007).
- ⁷ M. J. Rosenbluth, W. A. Lam and D. A. Fletcher, *Lab Chip*, **8**, 1062-1070 (2008).
- ⁸ H. Fujiwara, T. Ishikawa, R. Lima, N. Matsuki, Y. Imai, H. Kaji, M. Nishizawa, T. Yamaguchi, *J. Biomech.*, **42**, 838-843 (2009).
- ⁹ S.S. Lee, Y. Yim, K.H. Ahn, S. J. Lee, *Biomed. Microdev.*, **11**, 1021-1027 (2009).
- ¹⁰ V. I. Furdul, J. K. Kariuki and D. J. Harrison, *J. Micromech. Microeng.*, **13**, S164-S170 (2003).
- ¹¹ S. Böhm, W. Olthuis and P. Bergveld, *Biomed. Microdev.*, **1**, 121-130 (1999).

- ¹²Y.-C. Hsu, S.-J. Lin and C.-C. Hou, *Microsyst. Technol.*, **14**, 31-41 (2007).
- ¹³X. Chen, D. F. Cui, C.-C. Liu, and H. Li. *Sens. Actuators, B*, **130**, 216-221 (2008).
- ¹⁴Z. Wu, B. Willing, J. Bjerketorp, J.K. Jansson, K. Hjort, *Lab Chip*, **9**, 1193-1199 (2009).
- ¹⁵J. N. Lee, X. Jiang, D. Ryan, G. M. Whitesides, *Langmuir*, **20**, 11684-11691 (2004).
- ¹⁶T. T. Nguyen, M. Pharm, N. S. Goo, *Journal of Bionic Engineering*, **5**, 135-141 (2008).
- ¹⁷S.-H Chiu, C.-H Liu, *Lab Chip*, **9**, 1524-1533 (2009).
- ¹⁸I. D. Johnston, J. B. Davis, R. Richter, G. I. Herbert and M. C. Tracey, *Analyst*, **129**, 829-34 (2004).
- ¹⁹T. Goettsche, J. Kohnle, M. Willmann, H. Ernst, S. Spieth, R. Tischler, S. Messner, R. Zengerle and H. Sandmaier, *Sens. Actuators, A*, **118**, 70-77 (2005).
- ²⁰I. D. Johnston, M. C. Tracey, J. B. Davis and C. K. L. Tan, *J. Micromech. Microeng.*, **15**, 1831-1839 (2005).
- ²¹M. C. Tracey, I. D. Johnston, J. B. Davis and C. K. L. Tan, *J. Micromech. Microeng.*, **16**, 1444-1452 (2006).
- ²²I. D. Johnston, M. C. Tracey, J. B. Davis and C. K. L. Tan, *Lab Chip*, **5**, 318-325 (2005).
- ²³B. D. Iverson, S. V. Garimella, *Microfluid. Nanofluid.*, **5**, 145-174 (2008).
- ²⁴M. C. Tracey, I. D. Johnston, J. B. Davis and C. K. L. Tan, *The Institution of Engineering and Technology Seminar on MEMS Sensors and Actuators*, London, 2006.
- ²⁵H. Andersson, W. van der Wijngaart, P. Nilsson, P. Enoksson and G. Stemme, *Sens. Actuators, B*, **72**, 259-265 (2001).
- ²⁶A. Miller, M. Green, O. Robinson, *Brit. Med. Journ.*, **286**, 266 (1983).
- ²⁷L. T. Sniegoski, J. R. Moody, *Anal. Chem.*, **51**, 1577-1578 (1979).
- ²⁸A. Zwart, O. W. van Assendelft, B. S. Bull, J. M. England, S. M. Lewis and W. G. Zijlstra, *J. Clin. Pathol.*, **49**, 271-274 (1996).
- ²⁹*Guidelines on Standard Operating Procedures for HAEMATOLOGY*, World Health Organisation, 2006, ch. 7.
- ³⁰E. J. van Kampen, W. G. Zijlstra, *Clin. Chim. Acta*, **6**, 538-544 (1961).
- ³¹G. Su, R. M. Pidaparti, *Microsyst. Technol.*, **16**, 595-606 (2010).
- ³²N.-T. Nguyen, S. T. Werely, *Fundamentals and Applications of Microfluidics*, (Artech House Publishers, Boston, 2002).
- ³³F. Amirouche, Y. Zhou, T. Johnson, *Microsyst. Technol.*, **15**, 647-666 (2009).
- ³⁴M. Kersaudy-Kerhoas, R. Dhariwal, M.P.Y. Desmulliez, L. Jouviet, *Microfluid Nanofluid.*, **8**, 105-114 (2009).
- ³⁵J. J. Bray, P. A. Cragg, A. D. C. Macknight, R. G. Mills, D. W. Taylor, *Lecture Notes on Human Physiology*, 3rd ed. (Blackwell Scientific Publications, Oxford, 1994).
- ³⁶T. W. Secomb, *Cell Biophysics*, **18**, 231-251 (1992).